International Journal of Bioelectromagnetism
Vol. 13, No. 4, pp. 173-177, 2011

EEG Surface Laplacian using realistic head geometry

Siyi Deng, William Winter, Samuel Thorpe, Ramesh Srinivasan[a]
[a]*Dept. Cognitive Sciences, University of California, Irvine, USA*
Correspondence: Siyi Deng, Cognitive Sciences, University of California, Irvine, USA, CA 92697-5100
E-mail: sdeng@uci.edu, phone +1 949 824 2684

Abstract. This paper describes a new algorithm for computing the surface Laplacian of scalp potential using realistic head geometry reconstructed from MRI scans. This method improves the accuracy of surface Laplacian over regions where the surface geomtery deviates significantly from a sphere. Simulations and experimental data are presented to demonstrate the improvement of the proposed method over the conventional spherical method..

Keywords: EEG, Surface Laplacian, spatial filter, cortical potential, MRI

1. Introduction

The spatial resolution of EEG, or the ability to distinguish small spatial details from EEG, is limited by the volume conduction of current through the brain to scalp, due to the spatial smearing effect of the poorly conductive skull layer. There are diminishing returns for increasing the number of spatial samples (electrodes), and the transfer function converges rather quickly [Nunez and Srinivasan, 2006]. A volume conduction model of the head can be used with different source localization methods, but these model-based spatial analyses are also fundamentally limited. Currently most mathematical models of volume conduction rely on assumptions that oversimplify the nature of the problem. For instance, traditionally a 3 or 4-layer volume conductor is used to model the head, and within each layer the electrical property is assumed to be identical or follow some simple functions; there is a trade-off between introducing more layers and numerical stability of the mathematical solutions; in addition, the electrical property of head tissues in vivo is very difficult to model [Nunez and Srinivasan, 2006]. These limitations provide motivation for methods of improving EEG spatial resolution making minimal assumptions about tissue properties in realistic heads. The surface Laplacian of scalp potential (or second spatial derivative in two surface coordinates) is an estimate of current density entering (or exiting) the scalp through the skull. It requires only that the outer surface shape of the volume conductor be specified and does not require any details about volume conduction except for a poorly conducting skull. In simulations using spherical models, it has been demonstrated that the surface Laplacian closely approximates the potential at the boundary between the brain and skull [Srinivasan et al., 1996], and in applications to EEG data, the surface Laplacian is consistent with model based estimates of cortical surface potential [Nunez et al., 1994].

Traditionally, the surface Laplacian is computed by mapping the EEG onto a spherical surface to simplify calculating spatial derivatives. Methods based on parametric surface fitting and curvilinear coordinate transformations have also been proposed [Babiloni et al., 1996; He et al., 2001]. We have developed a new algorithm of computing the surface Laplacian for realistic head geometry directly on a trangulated mesh reconstructed from MRI scans. We present the general form of our realistic SSL, and show that for spherical surfaces it closely approximates the analytic result. We present simulations and experimental data to demonstrate the improvement of our method over the spherical approximation on ellipsoidal and realistic surfaces.

2. Spline surface Laplacian based on realistic geometry

The first step of the SSL-Geo algorithm is to construct a continuous potential distribution function from the discrete measurement form EEG electrode using a three dimensional polyharmonic spline interpolation scheme, identical to the spherical spline Laplacian [Nunez and Srinivasan, 2006].

The 3D polyharmonic spline is given by

$$V(x,y,z) = \sum_{i=1}^{n} pK_{m-1} + Q_{m-1} \tag{1}$$

where K_{m-1} is a radial basis function:

$$K_{m-1} = (d^2 + w^2)^{\mathrm{m}-1} \log(d^2 + w^2) \tag{2}$$

d is the Euclidean distance between the interpolation position and the sampling position, w is a constant coefficient that ensures the differentiability of the surface, and the Q_m is a m^{th} order polynomial acts to smooth the function; we set $m = 3$ and solve for p and q.

In the next step, the surface Laplacian operator is applied to the spline function previously constructed according to the following definition:

$$-\nabla_S^2 V = \mathrm{tr}[\nabla(I - \vec{n}^{\mathrm{T}}\vec{n})\nabla \mathrm{V}] \tag{3}$$

The surface normal part of the gradient of V is removed before calculating the divergence, defining a surface Laplacian. The quantity $I - \vec{n}^{\mathrm{T}}\vec{n}$ gives the projection onto the tangent plane at location r of unit surface normal $\vec{n}$. On most surfaces, this quantity is also a function of r and the partial derivative of $I - \vec{n}^{\mathrm{T}}\vec{n}$ reflects the impact of local geometry on the estimation of surface Laplacian.

After expanding the right hand side of Eq. 3, we obtain

$$-\nabla_S^2 V = \mathrm{tr}(\nabla\nabla V) - \vec{n}(\nabla\nabla V)\vec{n}^{\mathrm{T}} - \vec{n}\,[\mathrm{tr}(\nabla\vec{n})]\nabla V - (\nabla V)^{\mathrm{T}}(\nabla\vec{n})\,\vec{n}^{\mathrm{T}} \tag{4}$$

In the special case of a unit sphere, Eq. 4 can be analytically expressed as:

$$-\nabla_S^2 V = (x^2-1)\partial_{x,x}^2 V + (y^2-1)\partial_{y,y}^2 V + (z^2-1)\partial_{z,z}^2 V + 2xy\partial_{x,y}^2 V + 2xz\partial_{x,z}^2 V + 2yz\partial_{y,z}^2 V + 4x\partial_x V + 4y\partial_y V + 4z\partial_z V \tag{5}$$

which is the formulation of conventional spherical spline Laplacian (SSL-Sph).

In most realistic applications, such as the head model derived from MRI scans, it is difficult or impossible to obtain a parametric representation of the surface; the surface is usually discretized into a triangular mesh representation. On such general surfaces, the unit surface normal $\vec{n}$ and the curvature tensor (Jacobian matrix) $\nabla\vec{n}$ must be computed by means of discrete differential geometry. The unit normal at each vertex can be estimated from the surrounding triangle face normals, while the Jacobian matrix must be solved form the finite difference of vertex positions and normals.

3. Numerical Simulations

To investigate the effect of local changes in geometry (captured in the curvature tensor) on the accuracy of spline surface Laplacian, we implemented 3-shell confocal ellipsoidal volume conductors of various eccentricities. We kept the left-right and dorsal-ventral semi-minor axes identical and only vary the aspect ratio of posterior-anterior semi-major axis from 0.8 to 1.5, which corresponds to oblate (<1) and prolate (>1) spheroids. In the case of a sphere, the radii of the brain, skull and scalp boundary are set to 90, 95 and 100 mm, respectively and the conductivities are set to 0.33, 0.083 and 0.33 (sm^{-1}), which corresponds to a conductivity ratio of 40 between brain and skull. We used boundary element methods (BEM) to solve for the scalp and cortical (brain/skull boundary) potentials [Stenroos et al. 2007]. Dipole sources with random location and orientation are placed at least 10 mm under the brain ellipsoid surface. For each eccentricity level we performed 200 simulations. Since there is no practical analytical solution of the surface Laplacian for ellipsoidal volume conductors, we evaluated the performance of SSL-Geo and SSL-Sph by measuring the correlation between the spatial patterns of the surface Laplacian with the corresponding distribution of cortical potential (potential at the brain/skull boundary). In spherical models, the surface Laplacian is highly correlated with cortical potential [Nunez et al., 1994], as was confirmed by the simulations presented here. Figure 1 for shows that as the semi-axis ratio deviates from 1 (a sphere), both prolate (ratio > 1) and oblate spheroids (ratio < 1) show poorer performance for the SSL-Sph compared to SSL-Geo.

We then use a realistically shaped 3 layer BEM head model, reconstructed from MRI scans, to demonstrate that surface Laplacian effectively reduces the blurring of scalp measurement caused by a poorly conductive skull layer. 20 radial dipoles of random magnitude were placed 8 mm under the innermost layer (brain-skull boundary), and scalp potential were measured from 128 electrodes. After applying the SSL-Geo algorithm, we back-projected the resulting scalp surface Laplacian to the innermost layer, using a nearest neighbor criterion, to visually compare the distribution with cortical potentials measured at this layer. The result suggests that surface Laplacian of scalp EEG closes resembles the cortical potentials that may be recorded via EcoG devices, practically improved the spatial resolution of EEG by de-blurring the volume conduction effect. See figure 2 for details.

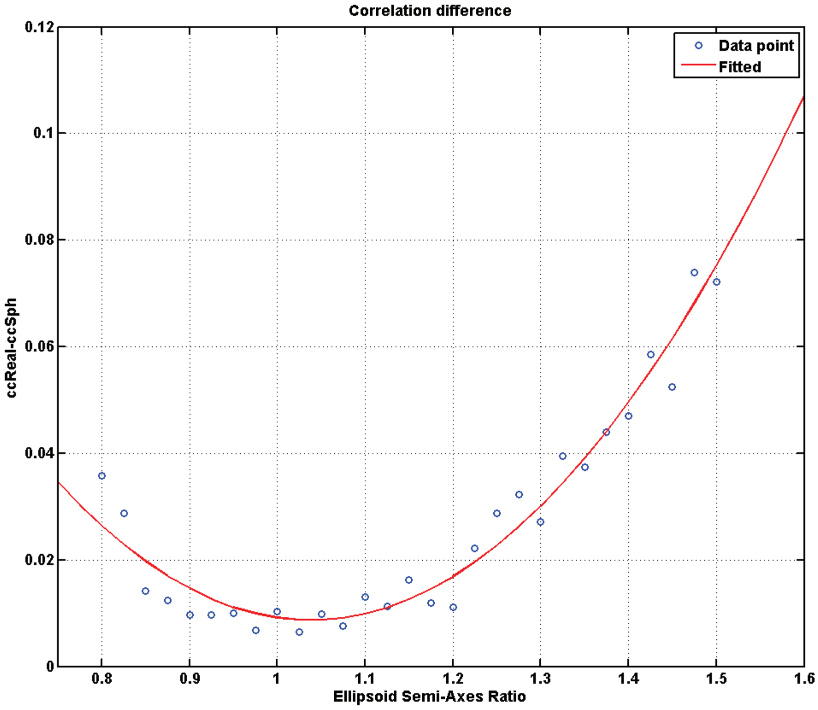

Figure 1. The improvement of the SSL-Geo over SSL-Sph on ellipsoidal surfaces. *The x-axis is given by the semi-major and semi-minor axis ratio. The y-axis is the difference of correlation coefficient when SSL-Geo and SSL-Geo are compared with the potential distribution on the cortical layer of the BEM volume conductor. Each data point represents the mean value of 200 simulations of 100 random dipolar sources. The fit curve is a quadratic polynomials.*

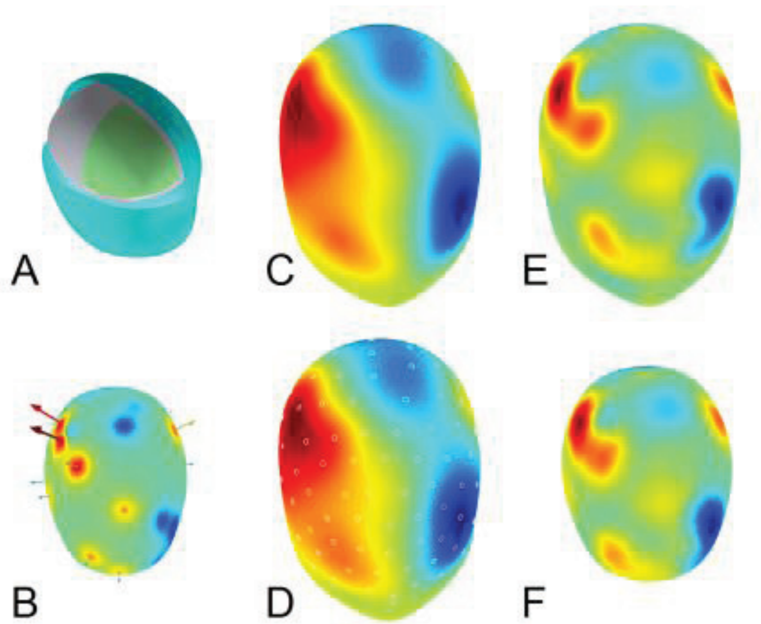

Figure 2. Scalp surface Laplacian and cortical potentials. *A. The 3-layer (cortex, skull, scalp) BEM model used in this simulation. B. 20 radial dipoles are place underneath the innermost layer, and the topographic distribution of the potentials that are measured on cortical surface. C. The scalp potenial computed using BEM. D. Spline interpolated scalp potential from 128 electrodes. E. The outcome of appling SSL-Geo to D. F. The result of E. back-projected onto the cortical surface. Notice the similarity between the topographic distribution in F and B.*

4. Experiments

We examined EEG data from one human subject attending to flickering visual stimuli on a computer screen. This paradigm is widely used (e.g., Srinivasan et al. 1999) to generate steady-state visual evoked potentials (SSVEPs) at occipital, parietal, and frontal areas in the brain. SSVEPs depend strongly on the flicker frequency; at higher frequencies (>15 Hz) SSVEP responses appear restricted to electrodes over occipital and parietal cortex, while at lower frequencies in the theta/alpha band SSVEP responses are also observed over frontal cortex [Ding et al., 2006]. In this specific experiment, one stimulus is flickering at 30 Hz over the right visual field of the subject, while another stimulus of 20 Hz is over the left, so we expect a lateralized and relatively localized response over the contralateral visual areas of the brain. There are two experimental conditions; the subject is instructed to attend to either the left or the right flicker, and perform a target detection task, while ignoring the other flicker (which also contains targets). For our purposes of testing the SSL-Geo we averaged the data over attention instructions. There are 12 trials each 30 seconds long for each condition. The EEG is recorded using a 128-channel Geodesic Sensor Net (Electrical Geodesics, Eugene, OR). The data was collected with a 50 Hz hardware lowpass filter and digitized at a 1000 Hz. The reference electrode is on the vertex; after identifying 7 channels likely containing artifact, the remaining 121 channels were average referenced. After preprocessing, SSVEPs are identified by applying the FFT to the EEG data to estimate power at exactly the two flicker frequencies (20 and 30 Hz). We apply both SSL-Geo and SSL-Sph directly to the Fourier coefficients to demonstrate the improvement of SSL-Geo by utilizing a more accurate model of scalp geometry. The results of 30Hz condition are shown in Figure 3. From the topographic distributions, it is clear that using surface Laplacian effectively improved the spatial resolution of the evoked potentials, and the proposed method has the advantage of higher signal to noise ratio over regions where the surface geometry deviates away from a sphere. It should be noted that the main difference in these plots is the widespread noise evident in the SSL-Sph as compared to the SSL-Geo. When amplitude criteria are used to detect peaks in the topography, SSL-Sph gives the false sense of additional peaks due to the widespread overestimation.

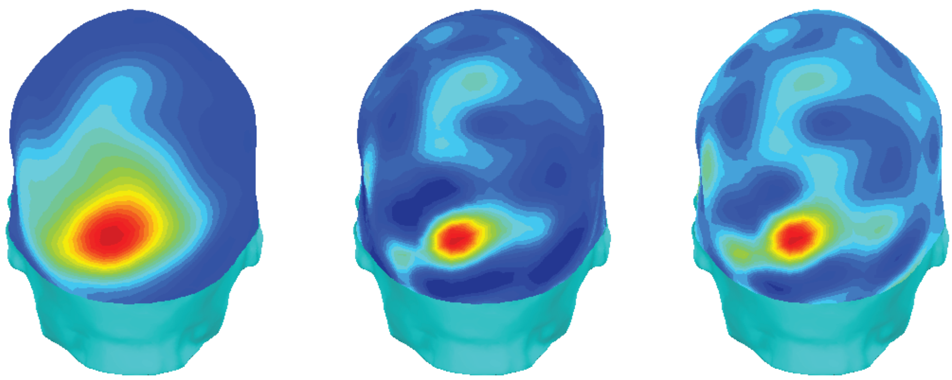

Figure 3. ***Topographic distribution of 30Hz SSVEPs and the corresponding surface Laplacians.*** *SSVEP elicited by the 30 Hz flicker is distributed primarily over the left occipital region. Applying SSL to the SSVEP effectively reduces the spatial blurring caused by volume conduction and increases spatial resolution. Compared to SSL-Geo, SSL-Sph has a pattern of widely spread overestimation which reduces the signal to noise ratio of the outcome.*

The SSL-Geo algorithm we have developed is a computational efficient estimator of the surface Laplacian on realistic scalp surfaces derived from MRI. Both our simulations and applications to realistic data indicate improvement in performance over the conventional spherical spline Laplacian. The strength of this approach is that an accurate volume conduction model, which is currently not available, is not required to detect source regions with accuracy on the 1-2 cm scale in surface tangential directions. The only limitation of the surface Laplacian is it insensitivity to deeper sources which generate widespread potentials.

To facilitate the adoption of both spherical Laplacians and our new SSL-Geo method, we have developed a MATLAB based toolbox called SSLTool that implements both algorithms. The toolbox can be found at http://hnl.ss.uci.edu/downloads.html

References

Babiloni F, Babiloni C, Fattorini L, Carducci F, Onnorati P, and Urbano A Performances of surface Laplacian Estimators: A study of simulated and Real scalp potential distributions; Brain Topography, Vol. 8, No. 1, pp. 35-45, 1995.

Ding J, Sperling G and Srinivasan R Attentional modulation of SSVEP power depends on the network tagged by the flicker frequency. Cereb. Cortex, Vol. 16, No. 7, pp 1016, 2006.

He B, Lian J and Li G High-resolution EEG: a new realistic geometry spline Laplacian estimation technique Clinical Neurophysiology Vol. 112, No. 5, pp 845, 2001.

Nunez P, Siberstein R, Cadusch P, Wijesinghe R, Westdorp A and Srinivasan R A theoretical and experimental study of high resolution EEG based on surface Laplacian and cortical imaging. Electroencephalography and Clinical Neurophysiology, Vol. 90, No. 1, pp 40, 1994.

Nunez P. and Srinivasan R Electric Fields of the Brain. 2nd Edtion, Oxford University Press, 2006.

Srinivasan R, Nunez P, Tucker D, Silberstein R and Cadusch P Spatial sampling and filtering of EEG with spline Laplacians to estimate cortical potentials. Brain topography, Vol. 8, No. 4, pp. 355, 1996.

Stenroos M, Mantynen V, and Nenonen J A Matlab library for solving quasi-static volume conduction problems using the boundary element method, Computer Methods and Programs in Biomedicine, No. 88, pp. 256-263, 2007.